Electronic Supplementary Information

Summary of II-IV-V$_2$ properties

Table S1 Experimental electronic & optical properties of II-IV-V$_2$ compounds. Forbidden transitions are shaded in red. All band gaps are for chalcopyrite phases. Experimentally determined chalcopyrite lattice parameters (a & c) are in Å, band gaps (E_g^{exp} from experiment and E_g^{calc} from our GW calculations) in eV, mobilities (μ) in cm^2/V s and free carrier concentrations (n & p) in cm^{-3}.

ID	Material	a	c	c/a	E_g^{exp} (E_g^{calc})	μ_e	n	μ_h	p	References
0	Si	5.43	—	—	1.12	< 1500	10^{14}-10^{19}	< 500	10^{14}-10^{19}	93
1	ZnSiP$_2$	5.40	10.44	1.93	2.0-2.3 (2.09)	50-1,000	10^{13}-10^{18}	1-25	$\leq 10^{17}$	11,12,19–26,33
2	ZnGeP$_2$	5.49	10.80	1.97	1.8-2.3 (2.10)	—	10^{13}-10^{15}	20	10^{10}-10^{17}	10–12,22,26,33
3	ZnSnP$_2$	5.65	11.30	2	1.6-2.1 (1.86)	—	—	55	10^{16}-10^{17}	5,10,12,22,33,53
4	MgSiP$_2$	5.72	10.11	1.77	2.2 (2.25)	—	—	—	—	25,94
5	CdSiP$_2$	5.68	10.44	1.84	2.2 (2.10)	200-1,000	10^{10}-10^{15}	—	—	11,12,22,25,33
6	CdGeP$_2$	5.77	10.82	1.88	1.6-1.8 (1.91)	100	10^{11}-10^{14}	25	10^{10}-10^{15}	10–12,22,33
7	CdSnP$_2$	5.90	11.52	1.95	1.0-1.5 (1.33)	2,000	10^{15}-10^{18}	—	10^{14}	10–12,22,33
8	ZnSiAs$_2$	5.61	10.88	1.94	1.7-2.1 (1.53)	40	10^{8}	140-170	10^{13}-10^{17}	6,10–12,22,25,33
9	ZnGeAs$_2$	5.67	11.15	1.97	0.6-1.1 (1.21)	—	—	55	10^{16}-10^{19}	7,10,12,33
10	ZnSnAs$_2$	5.85	11.70	2.00	0.6-0.7 (0.89)	—	10^{15}	300	10^{17}-10^{21}	12,22,33
11	MgGeAs$_2$	5.66	—	—	— (1.82)	600	10^{18}	35	10^{19}	95
12	CdSiAs$_2$	5.88	10.88	1.85	1.5-1.6 (1.57)	—	10^{17}	500	10^{14}-10^{17}	11,12,22,25,33
13	CdGeAs$_2$	5.94	11.22	1.89	0.5-0.6 (0.70)	2,500	10^{16}-10^{18}	1,500	10^{16}-10^{18}	12,33
14	CdSnAs$_2$	6.09	11.94	1.96	0.3 (0.38)	12,000	10^{17}-10^{18}	190	10^{17}-10^{18}	12,22,33,96

Stability of Photoelectrodes

The stability of n-type semiconductors under aqueous anodic conditions has been a challenge for many photoelectrochemical applications (e.g. solar water splitting). The aqueous Fe(CN)$_6^{(3^-/4^-)}$ system has been used to monitor the water stability of many semiconductor anode materials with and without different protection layers.[74,99,100] When ZnSiP$_2$ electrodes were tested under aqueous conditions for long periods of time (2-8 hours), some dissolution of the semiconductor was observed by scanning electron microscopy (SEM) and the photocurrent was observed to decrease slightly while the open circuit potential (E_{oc}) remained relatively constant. To confirm that the dissolution current of the ZnSiP$_2$ was negligible, an electrode was also tested in a non-aqueous electrochemical cell using the ferrocene/ferrocinium (Fc$^{+/0}$) redox couple (10 mM ferrocene, 0.05 mM ferrocinium, LiClO$_4$ supporting electrolyte in dry acetonitrile).[85] The photocurrent was very similar (within 10%) between the aqueous (50/350 mM Fe(CN)$_6^{3-/4-}$) and non-aqueous measurements; this is consistent with the expected photon flux through the solution being nearly the same (within 1%) in each case. This similarity in photocurrent confirms that dissolution was not a significant component in the J-E photoresponse observed for ZnSiP$_2$ electrodes under aqueous conditions.

ZnSiP$_2$ Single Crystal XRD Results

Table S2 Atomic coordinates and site occupancies for ZnSiP$_2$.

Atom	Wyckoff site	x	y	z	Occupancy	U_{eq} (Å^2)
Zn	4a	1/2	0	3/4	0.99(2)	0.005(1)
P	8d	0.73023(6)	1/4	1/8	1.00(2)	0.005(1)
Si	4b	0	0	1/2	1.00(2)	0.005(1)

Table S3 Crystallographic data for ZnSiP$_2$.

Item [units]	Value
Formula	ZnSiP$_2$
Space group	I$\bar{4}$2d (No.122)
Crystal system	Tetragonal
a [Å]	5.3986(2)
c [Å]	10.4502(6)
V [Å^3]	304.57(2)
Z	4
FW [g/mol]	155.413
ρ_{calcd} [g/cm^3]	3.389
Atomic density [atoms/cm^3]	5.25×10^{22}
T [K]	293(2)
λ [Å]	0.71073
$\theta_{maximum}$	49.81
Number unique reflections (n)	798
Number reflections I $>2\sigma$(I)	726
Number of refined parameters (p)	11
Extinction coefficient	0.046(2)
μ [mm^{-1}]	9.18
Flack parameter	0.023(6)
$R(int)$ [%]	1.93
$R(F)^{\text{a}}$[%]	1.71
$Rw(F_o^2)^{\text{b}}$[%]	3.79
$GOF(F^2)^{\text{c}}$	1.099
$\Delta\rho_{min}$, $\Delta\rho_{max}$	-1.198, 0.583

$^{\text{a}}$ $R(F) = \Sigma \left| |F_o| - |F_c| \right| / \Sigma |F_o|$

$^{\text{b}}$ $Rw(F_o^2) = \left[\Sigma w (F_o^2 - F_c^2)^2 / \Sigma w (F_o^2)^2 \right]^{1/2}$

$^{\text{c}}$ $GOF(F^2) = \left[\left(\Sigma \left| w / \left| F_o^2 - F_c^2 \right|^2 \right| \right) / (n - p) \right]^{1/2}$

Table S4 Anisotropic displacement parameters for ZnSiP$_2$.

Atom	U_{11}	U_{22}	U_{33}
Zn	0.00463(5)	0.00463(5)	0.00522(6)
P	0.00481(9)	0.00455(8)	0.0045(10)
Si	0.0046(1)	0.0046(1)	0.0042(1)

Table S5 Selected bond distances (Å) and angles (°) for ZnSiP$_2$.

Configuration	Distance	Configuration	Angle
Zn-P ($\times$4)	2.3767(2)	P-Zn-P ($\times$2)	107.582(3)
		P-Zn-P ($\times$2)	113.320(7)
Si-P ($\times$4)	2.2522(2)	P-Si-P ($\times$2)	109.102(7)
		P-Si-P ($\times$2)	109.656(4)

In the SiP$_4$ tetrahedra, P-Si-P angles measure 109.102(7)° and 109.656(4)°, which are close to the ideal 109.5° angles expected for tetrahedral geometry. In ZnP$_4$, however, two of the angles measure 107.582(3)° while two angles measure 113.320(7)°, which indicate a distorted tetrahedral Zn environment.

Non-Dimensional Form of DAP Time Dependent Equations

The non-dimensional variable, $x \equiv r^3 N$, and parameter, $\zeta \equiv a^3 N$, are defined from r, the distance between DAP's, a, the characteristic distance (attributed to the larger of the donor or acceptor effective Bohr radii[56]), and N, the concentration of the majority defect. The recombination rate as a function of x is then

$$W(x) = W_0 \, exp\left[-2 \, (x/\zeta)^{1/3}\right], \tag{S1}$$

where W_0 is the rate as $r \to 0$, as it is in Eqn. 2. Given that $x = r^3 N \to dx = 3\,r^2 N\,dr \to r^2\,dr = \frac{dx}{3\,N}$, the PL intensity as a function of time, t, according to Eqn (3), but in terms of x instead of r, is proportional to

$$I(t) \propto exp\left[\frac{4}{3}\pi\int_0^\infty \left(exp\left[-W(x)\,t\right]-1\right)dx\right] \times \frac{4}{3}\pi\int_0^\infty W(x)\,exp\left[-W(x)\,t\right]\,dx, \tag{S2}$$

Intrinsic Point Defect Formation Enthalpies

Doping of many wide-band gap semiconductors has proven to be challenging.[97] Figure 4 (a) shows a heat map of E_F, which is determined by the charge balance between the predominant donor and acceptor point defects. The Fermi level lies above mid-gap over the majority of the single phase region where ZnSiP$_2$ is stable, resulting in intrinsic to moderately n-type conductivity. This result is promising as many compound semiconductors suffer from degenerate conductivity. In fact, ZnSiP$_2$ has been synthesized as both n- or p-type material, likely due to impurities arising from the synthesis techniques. Crystals grown in a Zn flux have been reported with both n-type,[2,21,24,29,30,32] and p-type conductivity.[20,23,24,30] All reports of growth in Sn flux have been n-type.[11,21,23,24,28,30,32,35] Halogen assisted vapor transport growth with I has produced n-type crystals,[28,35] while use of Cl as the carrier gas, with ZnCl$_2$ and PbCl$_2$ as Cl sources, has produced p-type crystals.[20,23,24,98] There is one report of n-type conductivity resulting from Cl vapor transport using SiCl$_4$ as the Cl source.[21] The crystals have been intentionally, extrinsically doped n-type by adding Se, Te, In, or Ga, and p-type by adding Cu.[11,19,20,28,31] The electronic properties that have been reported in these and other studies are given in Table S1. When other elements are involved in the synthesis (Sn flux or I, or Cl vapor transport) they have been found as impurities in the resultant crystals.[35] These studies demonstrate that ZnSiP$_2$ can be synthesized either n- or p-type, using extrinsic dopants, with carrier concentrations acceptable for PV devices.
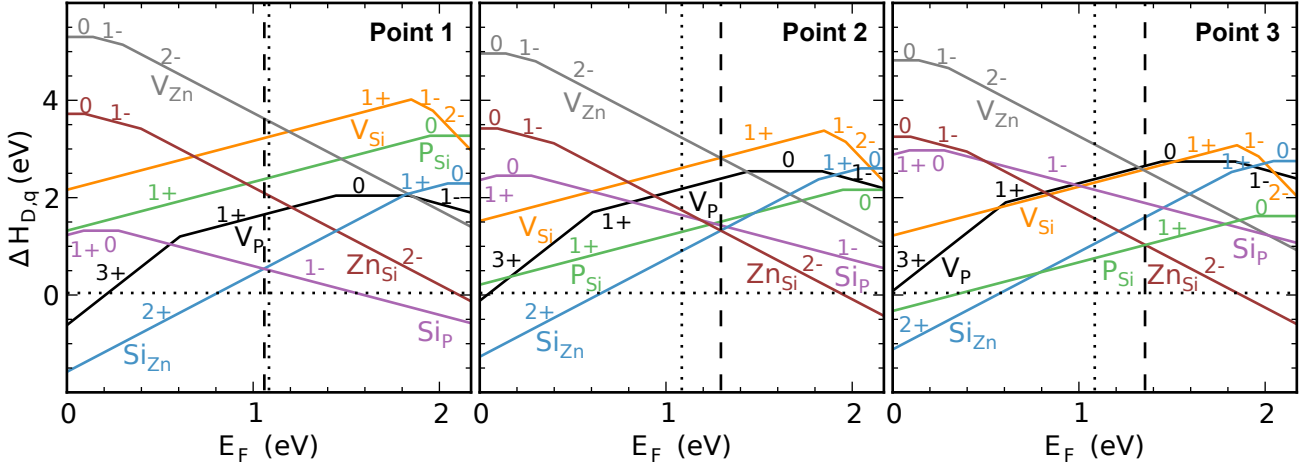

Fig. S1 Defect formation enthalpies ($\Delta H_{D,q}$) of 7 different point defects (vacancies and antisites) in all possible charge states (q ranging from 4- to 4+) at points 1, 2, and 3 on the phase diagram (a). The Fermi level is shown as a vertical dashed line along with mid-gap which is shown as a vertical dotted line.

References <small>(in addition to those given in the article)</small>

93 S. M. Sze and K. K. Ng, Physics of semiconductor devices, John Wiley & Sons, 3rd edn., 2006.

94 A. Springthorpe, R. Harvey and B. Pamplin, Journal of Crystal Growth, 1969, 6, 104–106.

95 Z. Li, H. Bender, M. Malfait, V. V. Moshchalkov, G. Borghs and W. V. Roy, Physica Status Solidi (a), 2007, 204, 152–158.

96 A. Strauss and A. Rosenberg, Journal of Physics and Chemistry of Solids, 1961, 17, 278–283.

97 W. Walukiewicz, Physica B: Condensed Matter, 2001, 302, 123–134.

98 E. Ziegler, W. Siegel and A. Heinrich, physica status solidi (a), 1974, 24, K79–K83.

99 S. Hu, M. R. Shaner, J. A. Beardslee, M. Lichterman, B. S. Brunschwig and N. S. Lewis, Science, 2014, 344, 1005–1009.

100 M. R. Shaner, S. Hu, K. Sun and N. S. Lewis, Energy Environ. Sci., 2015, 8, 203–207.